

Probing the complex between the factor for inversion stimulation and DNA using a nanofluidic device

A novel method to study DNA protein complexes in vitro

Author:

Robin HAGMAN

Examiner:

Asst. Prof.
Fredrik WESTERLUND

Department of Chemical and Biological Engineering

CHALMERS UNIVERSITY OF TECHNOLOGY

Gothenburg, Sweden 2013

Master's Thesis 2013

The cover page picture shows a cartoon representation of the factor for inversion stimulation protein made with the program Jmol with information from NCBI - 1FIA.

Abstract

Every living cell on the planet uses DNA to store information. Some of this information is used to make proteins and also for cell division. Many processes in the cell are controlled and regulated by interactions between DNA and proteins. Nanofluidic devices with fluorescence microscopy have been used to study single DNA molecules for almost a decade and the purpose of this thesis was to investigate if this technique can be used to study interactions between DNA and proteins.

In order to do this, a small nucleoid protein called the Factor for Inversion Stimulation (FIS) was used as a model system. The nanofluidic device was coated with a lipid-bilayer to prevent the protein from sticking to the channel walls and the extension of the DNA-FIS complex was investigated in nanochannels to determine how the physical properties of DNA changed when FIS was bound.

The results showed that it was possible to study the extension of the DNA-FIS complex and a sequence specific binding to GC-rich regions, that seemed to be affected by salt concentration, was observed. The physical properties of DNA were shown to change when FIS was bound since the extension of the complex did not change in different salt concentrations. The decreased emission intensity from the DNA-FIS complex with time seemed to be due to bleaching of the dye and no dissociation of FIS could be confirmed.

This study shows that a nanofluidic device coated with a lipid-bilayer can be used to study a DNA associating protein. This was an initial study and one of the first times a DNA associated protein was studied in a nanofluidic device. More experiments need to be performed in order to better understand the DNA-FIS interaction.

Acknowledgements

I would like to thank the following people: Fredrik Westerlund for having me as a master student in this master's thesis project and for always being supportive. Karolin Frykholm for being an excellent laboratory supervisor and for helping me with the experiments. Gustav Emilsson, Jens Wigenius, Joachim Fritzsche, Lena Nyberg, Louise Fornander, Mohammadreza Alizadehheidari and Yuri Antonio Diaz Fernandez for all interesting talks and social activities. Mauro Modesti for providing the labelled proteins and Fredrik Persson for supplying the MATLAB program SMATool.

Robin Hagman, Gothenburg 2013-05-24

Contents

1	Introduction	1
1.1	Background	1
1.2	Purpose	2
2	Theory	3
2.1	Fluorescence Microscopy	3
2.2	Nanofluidic Devices	4
2.3	DNA	6
2.4	Protein Synthesis	7
2.5	Factor for Inversion Stimulation	8
2.6	Polymer Theory	8
2.7	Image Analysis	10
3	Materials and Methods	11
3.1	Chemicals	11
3.1.1	Dyes	12
3.1.2	Liposome Preparation	12
3.2	Protein	13
3.3	Preparation and Coating of the Nanofluidic Chip	13
3.4	Experiments with DNA-FIS Complexes in a Nanofluidic Device . .	14
3.4.1	Funnel and Straight Chip Experiments	14
3.4.2	Tandem and Interval Experiments	15
3.4.3	T4DNA Experiments	15
3.5	Preparation and Experiment with Label IT	15
3.6	Image Analysis	15
4	Results	17
4.1	Extension of DNA-FIS Complexes in Different Salt Concentrations .	17

4.1.1	Sequence Specific Binding of FIS	19
4.2	Extension of DNA-FIS Complexes in Different Confinements	20
4.3	The Intensity Problem, Bleaching and/or Dissociation?	22
4.4	Label IT to Covalently Label DNA	27
5	Discussion	28
5.1	Are the DNA-FIS Complexes Affected by Different Salt Concentra- tions?	28
5.2	Is a Sequence Specific Binding Distribution of FIS Detectable?	29
5.3	Can the Extension of a DNA-FIS Complex be Investigated in Dif- ferent Confinements?	29
5.4	Is the Intensity Drop Due to Bleaching and/or Dissociation of FIS?	30
5.5	Can Label IT be Used to Covalently Label DNA?	31
6	Conclusions	32
	Bibliography	34
	Appendices	37
A	Protein Purity	38
B	Rewritten deGennes Equation	39
C	MATLAB Intensity Profile Code	40

List of terms

Bleaching	Is when the emission intensity of a fluorescent dye molecule decreases due to damages caused by photons.
Chuck	A plastic device which is used as an interface between the nanofluidic chip and the user. It holds the chip and contains holes which are connected to the chip reservoirs and screws which are used to seal them off. Inlets for directing gas pressure to each reservoir are also present.
DTT	Dithiothreitol (DTT) is used as an oxygen scavenger which decreases the amount of reactive oxygen in the sample, which is of importance since reactive oxygen can react with DNA and damage it or cause bleaching.
Funnel chip	A silicon oxide chip which contains nanochannels with a constant depth of $140nm$ and a width that continuously decreases from $800nm$ to $100nm$.
Kymograph	Is a picture representation of a movie where the first frame in the movie is represented at the top of the picture and the last frame at the bottom.
Nanofluidic device	When the chip is mounted to the chuck it is referred to as a nanofluidic device, the metal plate and screws for mounting the chip on the chuck and sealing of the reservoirs are included as well.
Straight chip	A silicon oxide chip which contains nanochannels with a constant depth and width of $150nm$ and $100nm$ respectively.
TBE buffer	A buffer commonly used when working with nucleic acids, it contains Tris base $(HOCH_2)_3CNH_2$, Boric acid H_3BO_3 and EDTA (Ethylenediaminetetraacetic acid).

1

Introduction

THIS CHAPTER WILL describe why nanofluidic devices and fluorescence microscopy are of interest to study DNA-protein interactions, and how the Factor for Inversion Stimulation protein can be used as a model system for such a study. The purpose is described and the objectives are stated.

1.1 Background

Nanofluidic devices have been extensively used to study how single DNA molecules behave under strong confinement for almost ten years. These studies have given great insight into how DNA molecules behave when confined as well as how the physical properties of DNA changes in different environments (e.g. different salt concentrations). This has led to the development of powerful single molecule techniques to study different aspects of DNA [1, 2]. One practical example is that nanofluidic devices with fluorescence microscopy have recently been used to optically map DNA. This single-step method utilizes YOYO-1 and netropsin to optically map darker regions on the DNA to AT rich sequences and brighter regions to GC rich sequences [3]. This method could for example be useful for a quicker identification of different pathogens like bacteria and viruses at hospitals, compared to cell culturing techniques used today.

Usage of nanofluidic devices to study DNA-protein complexes is also of interest since many different types of proteins interact with DNA and these different DNA-protein interactions are of great importance for how the cell functions. For example, in most eukaryotes DNA associates to histones and forms a larger complex called chromatin that serves several functions, one of them is to pack DNA into chromosomes when cells divide. Another interesting aspect of chromatin is

the wide range of different post-translational modifications that can occur on the histone tails [4]. It might be a possibility that nanochannels could be used to study chromatin and post-translational modifications. Some benefits of using nanofluidic devices to study DNA-protein complexes are that the physical properties of complexes can be investigated, complexes do not need to be tethered to anything and they could potentially be directly extracted from one cell or a population of cells inside the chip [5]. Different types of proteins have previously been studied in nanofluidic devices e.g. a restriction enzyme [6] and a repressor protein [7]. This project was one of the first investigations where a nanofluidic device passivated with a lipid-bilayer was used to study the interaction between a nucleoid protein and DNA.

The Factor for Inversion Stimulation (FIS) is a nucleoid-associated protein from *Escherichia coli* which affects the physical properties of DNA. An earlier study has shown that FIS binds to specific structures and sequences on the *E. coli* chromosome [8]. The aspect of studying single DNA-FIS complexes with fluorescence microscopy could give some new insight into these interactions. In this work, it will be investigated if a nanofluidic device could be used to study fluorescently labelled FIS bound to DNA. As a first step it was important to understand how DNA-FIS behaves in the device and how it was affected by different spatial confinements and different salt concentrations.

1.2 Purpose

The purpose of the project was to investigate the interaction between DNA and FIS in nanofluidic devices and to lay the ground for the development of a method to study DNA-protein complexes in nanofluidic devices, which could be used for further biological investigations. Since little was known about these interactions a number of different aspects were initially investigated. During the initial investigations the emission intensity from FIS was observed to drop faster than expected, this was therefore investigated further. The objectives were to investigate the following:

- If the extension of a DNA-FIS complex could be determined in nanofluidic channels.
- If the DNA-FIS complex was affected by different salt concentrations and if a sequence specific binding of FIS was detectable.
- If the emission intensity drop was due to bleaching and/or dissociation of the protein.
- If Label IT could be used to covalently label DNA.

2

Theory

IN THIS CHAPTER the different techniques used will be presented to give a better understanding of how they were employed to perform the experiments. The basics of fluorescence microscopy and how it was used to detect molecules will be described. An explanation of what a nanofluidic device is and how it was used to probe the DNA-FIS interaction as well as a basic introduction to DNA and protein synthesis are presented. A description of the protein used in this study and an overview of polymer theory and image analysis are presented.

2.1 Fluorescence Microscopy

To visualize the DNA-protein complex in the nanofluidic device, fluorescence microscopy was utilized. Fluorescence microscopy uses the light emitted (fluorescence) by molecules when they go from an excited state S_1 , to the ground state S_0 (Figure 2.1a). In order to study this, the molecules first need to be excited from their ground state. This is done by using light at a wavelength that corresponds to the difference in energy between S_0 and S_1 . The energy absorbed excites the molecule to S_1 and excess energy is quickly transferred to the surrounding environment by non-radiative transitions (vibrational relaxation) so that the molecules end up in the lowest vibrational state in S_1 . It is then the energy difference from S_1 to S_0 that can be emitted as fluorescence when the molecule goes back to the ground state [9].

The fluorescence microscopy setup (Figure 2.1b) consists of a light source and an excitation filter to extract light with the specific wavelength that is used to excite molecules in the sample. The fluorescent light from the sample is then transferred through an emission filter to filter out light that does not have the

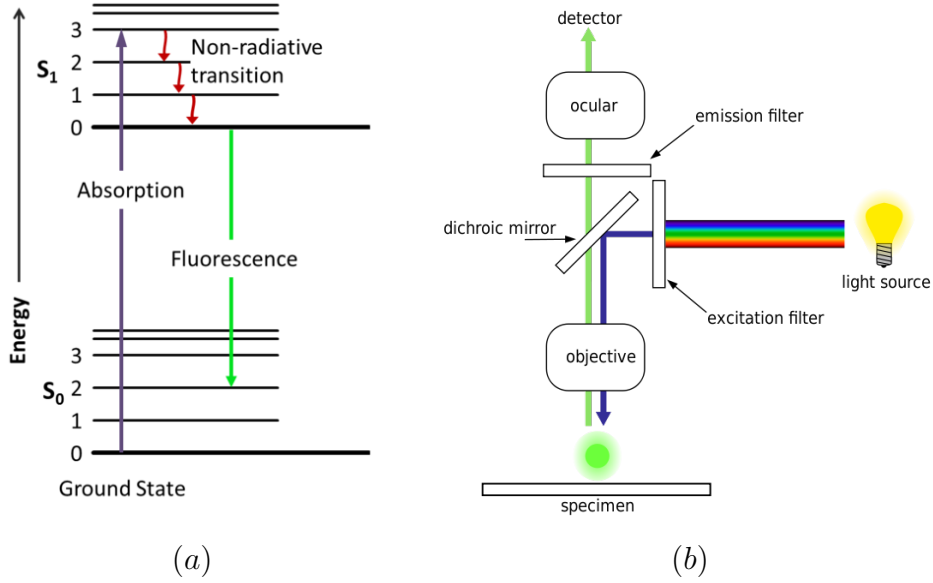


Figure 2.1: The Jablonski diagram [10] (a) describes the absorption of light that excites the molecule from its ground state S_0 to its excited state S_1 . The transitions within S_1 due to vibrations and fluorescence when the electron moves back to the ground state S_0 is shown. This diagram does not include internal conversion, inter-system crossing or phosphorescence since this thesis is focused on fluorescence. (b) Schematic setup for fluorescence microscopy [11].

desired wavelength before the light is passed through the ocular to the observer or through a side port where the emission can be detected using a sensitive EMCCD camera [4].

2.2 Nanofluidic Devices

In order to enable the study of single DNA-protein complexes in nanochannels a nanofluidic chip was used. Nanofluidic chips are often made in silicon oxide due to its ready availability and ease of use. The surface is negatively charged which is a problem when studying proteins since most DNA associating proteins are positively charged and therefore tend to stick to the channel. To circumvent this problem and enable DNA-protein complex investigation, the nanofluidic chip was coated with a lipid-bilayer [6].

The layout of the chip can be varied to address different issues, here 2 examples of a nanofluidic chip will be described (Figure 2.2). Both chips contain 4 reservoirs where fluid can be injected, they are then connected in pairs with microchannels,

reservoir B with C and A with D. A region between the 2 microchannels is then connected with several nanochannels to make the final structure of the nanofluidic chip. The first example (Figure 2.2a) is a "straight" chip where the nanochannels have a constant width and depth of $100nm$ and $150nm$ respectively. The second example (Figure 2.2b) is a "funnel" chip where the nanochannels in one end have a width of $800nm$ which continuously decreases to $100nm$ at the other end, the depth is constant at $140nm$.

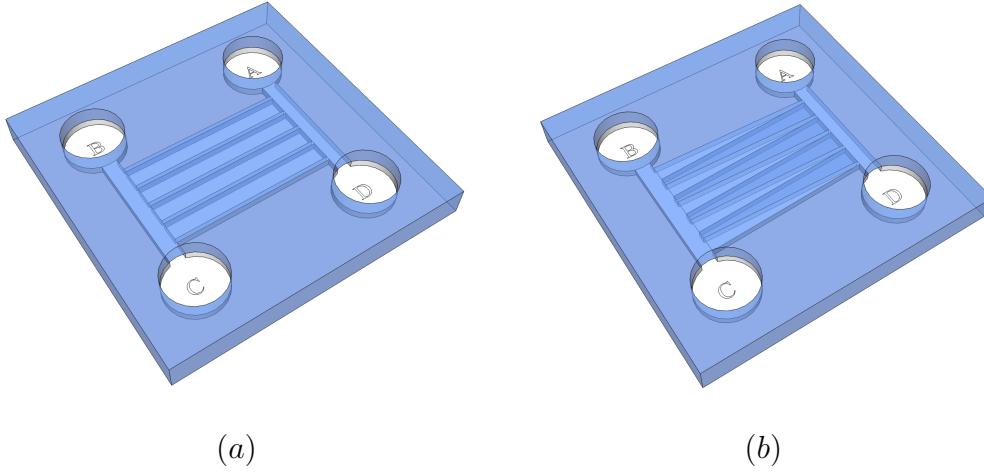


Figure 2.2: 2 types of nanofluidic chips, the reservoirs where the sample can be applied are labelled from A to D. In both types the reservoirs are connected in pairs with a microchannel (A with D and B with C) and between these microchannels are the nanochannels. Shown in (a) is the "straight" chip where the nanochannels have a constant width of $100nm$ and a depth of $150nm$. Shown in (b) is the "funnel" chip where the nanochannels have a width of $800nm$ from the BC side which then decreases continuously to $100nm$ on the AD side, the depth is constant at $140nm$. The difference in this illustration between the microchannel and nanochannel is not to scale, in reality, the nanochannel is around hundred times smaller than the microchannel.

In order to use the nanofluidic chip it needs to be mounted on a chuck which is a plastic device where screws can be used to seal off each reservoir. For each reservoir there are inlets to direct pressure from a pump or pressure container, this chuck and nanofluidic chip is what is referred to as a nanofluidic device. In order to analyse a sample of DNA-protein complexes, the channels need to be wetted with a buffer solution and coated with a lipid-bilayer (Section 3.3). Then, a sample of DNA-protein complexes can be added to one of the reservoirs, for example B, and by applying pressure at reservoir B and A the solution can be transferred to the microchannel. Once a sufficient number of complexes are in the microchannel

the pressure can be changed by applying pressure also on reservoir C so that the complexes move closer to the nanochannels connecting the 2 microchannels. Then, by only applying pressure on the microchannel where the DNA-protein complex is, reservoir B and C, the complex will be pushed into the nanochannel where it can be analysed by fluorescence microscopy. When the measurement of the confined complex is done, the pressure can be changed so that a new sample can enter the nanochannel and be analysed [2].

2.3 DNA

Every living cell on the planet contains DNA which is used to store information. This information is called the genetic code and is written in a four letter alphabet ATGC (Figure 2.3). Each letter denotes a base which is connected to a sugar phosphate group to form a nucleotide, these are then connected in an unbranched chain to make single stranded DNA (ssDNA). The bases (A)denine and (T)hymine

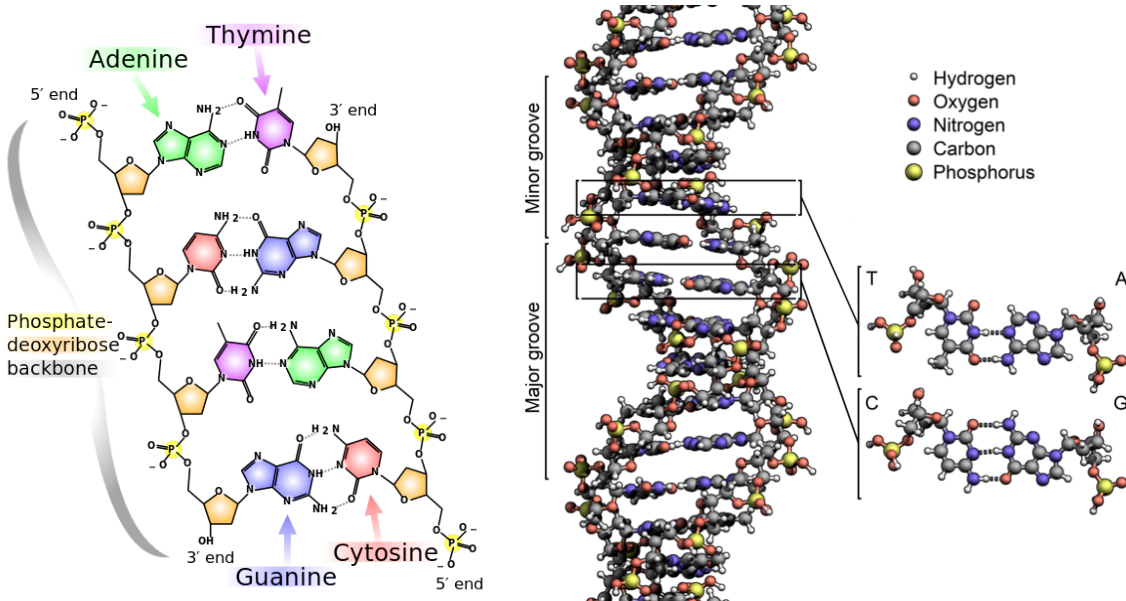


Figure 2.3: The structure of the DNA molecule, how the different nucleotides are connected and the shape of the DNA molecule with its major and minor groove [12].

can form base pairs with 2 hydrogen bonds while (G)uanine and (C)ytosine form base pairs with 3 hydrogen bonds, they are complementary. This entails that ssDNA can be used as a template for a complementary strand which, when bound together makes the double stranded DNA (dsDNA). Each ssDNA has a direction

since the sugar phosphate connecting the nucleotides (often referred to as the backbone) only can be connected to the 3' end. This directionality makes the two ssDNA molecules antiparallel in the dsDNA. From now on in this thesis, DNA refers to dsDNA. When cells divide they use proteins to replicate the DNA by using each complementary ssDNA as a template for the other so that both cells receive their own copy of DNA [4].

2.4 Protein Synthesis

The genetic code contains instructions for making all the different proteins that the cell needs to function and to make more copies of itself. In order to synthesise a protein (Figure 2.4), DNA is first copied to RNA (transcription) which is similar to DNA but the sugar is changed from a deoxyribose to a ribose and the base (T)hymine is exchanged with (U)racil. There are a variety of different types of

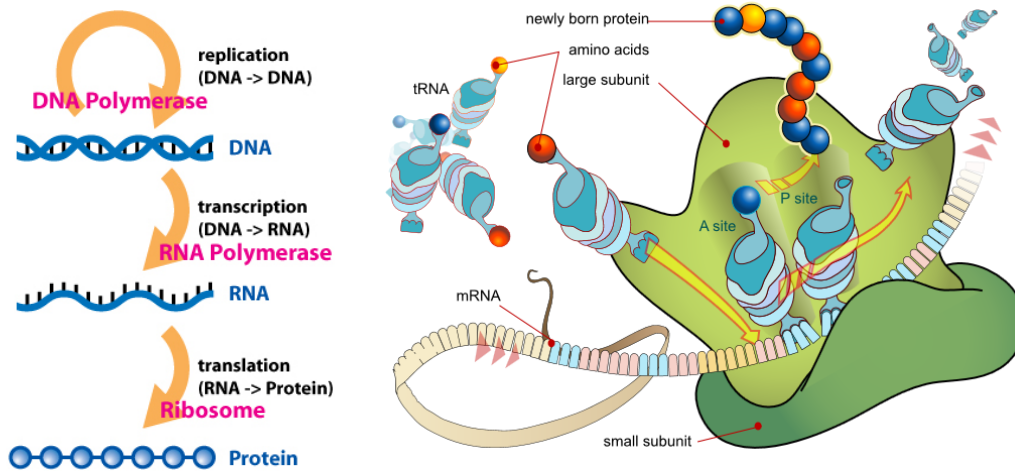


Figure 2.4: The central dogma of molecular biology (left): replication, transcription and translation [13]. Translation of mRNA (right) to a protein by the ribosome which consists of a small and large subunit [14].

RNA molecules, but the transcribed RNA for protein synthesis is called messenger RNA (mRNA). A protein complex called the ribosome then translates the 4 letter alphabet to the 20 letter alphabet of proteins by using the mRNA as a blueprint for protein synthesis (translation). This translation is done by matching 3 bases called a codon on the mRNA to a transfer RNA (tRNA) with the correct anticodon. For example, the codon UGG on the mRNA base pairs with the anticodon ACC on tRNA. This tRNA carries a specific amino acid (tryptophan) which is added to the newly born protein and the ribosome repeats the process of codon and anticodon

matching to link different amino acids together to form a protein. How the cell coordinates which protein that should be synthesised when is a very complicated process that involves many different protein-protein and DNA-protein interactions [4].

2.5 Factor for Inversion Stimulation

The Factor for Inversion Stimulation (FIS) (Figure 2.5) is a homo-dimer protein containing 2×98 amino acids and it is one of the 12 nucleoid proteins in *Escherichia coli*. FIS is the most abundant nucleoid protein during the growth phase of *E. coli* and between growth phases the concentration drops to undetectable concentrations [15]. The protein is named from being recognized as a factor for inversion stimulation but has later been found to be a versatile protein that can regulate replication, transcription, recombination and its own expression by binding a sequence motif of 2×15 base pairs on DNA. The protein binds non-specifically to DNA in the major groove in a helix-turn-helix manner and the binding is facilitated by 2×6 positively charged amino acids (Arginine, Lysine) [16]. The X-ray crystal structure was determined independently by 2 groups in 1991 [17, 18].

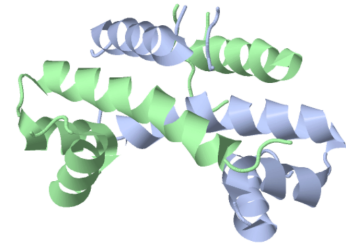


Figure 2.5: Cartoon representation of the 2×98 amino acid homo-dimer protein FIS, each dimer is shown in one of 2 colors.

It has been suggested that FIS can bind to DNA in a variety of ways; at lower concentrations the bound FIS on DNA are well separated from one another, each protein bends the DNA up to 90° and thereby compacts it slightly. At higher concentrations (DNAbp:FIS, 21:1) the protein covers the whole DNA molecule and there is less bending, about 50° , induced by each FIS protein which sit side-by-side of each other. At even higher concentrations (DNAbp:FIS, 21:2) the DNA-FIS complex forms a low mobility complex (LMC) which can form loops to further collapse the LMC [19]. This looping by FIS probably stabilizes the loop-domain structure of the *E. coli* chromosome [20]. Another interesting aspect of FIS is its higher affinity for GC rich regions compared to AT [8] which might be detectable in nanochannels.

2.6 Polymer Theory

When a DNA molecule is free in solution it contracts into a blob due to increased entropy in the blob state, but since DNA is negatively charged it tries to avoid

itself which increases the size of the blob. The radius of the blob can be described by the equation:

$$R = (P\omega_{eff})^{\frac{1}{5}} L^{\frac{3}{5}} \quad (2.1)$$

where R is the free-solution radius of gyration which can be viewed as the distance from the center of the blob to the rand. P is the persistence length which indicates the stiffness, ω_{eff} is the effective width and L is the contour length which is the physical maximum length of the extended DNA molecule [1].

Depending on the spacial confinement, 3 different theory's can be used to describe the behaviour of the DNA molecule (Figure 2.6). In the first case, the cross section area of the confinement (D) is larger than the radius of gyration (R) and the molecule behaves as in free solution (Equation 2.1). The second case is when the confinement is smaller than the radius of gyration but much larger than the persistence length (P). Then, the end-to-end distance (extension) of the molecule can be described by deGennes theory:

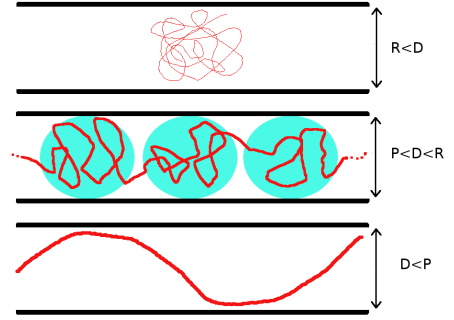


Figure 2.6: 3 different regimes for DNA in spacial confinements, adopted from [2]

$$\frac{r}{L} = \left(\frac{\omega_{eff}P}{D_{AV}^2} \right)^{\frac{1}{3}} \quad (2.2)$$

where r is the measured extension, L , P and ω_{eff} are as mention previously and D_{AV}^2 is the cross section area of the channel. In this regime the molecule behaves as a series of connected blobs where each blob behaves as in free solution (Equation 2.1). The third and last case is when the confinement is much smaller than the persistence length and the end-to-end distance can be described by Odijk theory:

$$\frac{r}{L} = 1 - B \left[\left(\frac{D_1}{P} \right)^{\frac{2}{3}} + \left(\frac{D_2}{P} \right)^{\frac{2}{3}} \right] \quad (2.3)$$

where r , L and P are the same as in deGennes equation, B is a proportionality constant numerically determined to ~ 0.091 [21], D_1 and D_2 are the width and height respectively of a rectangular nanochannel. In this regime the molecule undulates between the channel walls and does not form any loops as in the previous two cases. In both the deGennes and the Odijk equation, the measured extension (r) is directly proportional to the contour length (L) which means that a molecule that appears twice as extended, compared to another molecule, also has twice the contour length [2]. The transition between the deGennes and the Odijk regimes are not that well understood and unfortunately the $100 \times 150nm^2$ channels used in this work are close to where this transition takes place. To be considered within

the deGennes regime the boundaries needs to be changed to $P \ll D \ll R$ and for the Odijk regime to $D \ll P$. It has been suggested that in the transition state the DNA molecule partially folds back on itself to form small hairpin like structures [22]. For λ DNA, one type of DNA that was used in this work, typical values are $P = 50nm$, $\omega_{eff} = 5nm$ and $L = 16.5\mu m$ [23].

2.7 Image Analysis

After the DNA-FIS complex was confined in a nanochannel and imaged with an EMCCD camera, the images were processed into an average kymograph. In this example, 200 images were captured during 32s. By selecting a region of interest (ROI) around the complex (Figure 2.7), in this case with a height of 10 pixels and width of 147 pixels, a software program (ImageJ) can take the top pixel row from the ROI in each of the 200 images and produce a kymograph. The width of the kymograph was thus the width of the ROI (147 pixels) and the height of the kymograph represents the time (32s). The process was then repeated for the

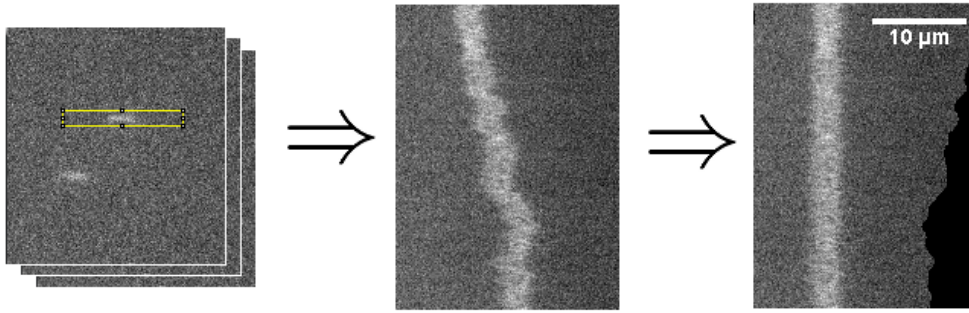


Figure 2.7: The work flow from a stack of images of a complex (left) to an average kymograph (middle) into a center aligned kymograph (right) which could be used to determine the complex extension and intensity over time. In this example 200 images were captured during a 32s measurement.

other 9 pixel rows and an average of 10 kymographs was calculated to produce one average kymograph. Then a MATLAB program (Section 3.6) was applied to calculate the width and center of the complex by investigating the intensity. The kymograph was then aligned so that the center of the imaged complex stays at the same position throughout the duration of the experiment. This center aligned kymograph was used to visualize how the molecule behaves during the measurement. It was also a confirmation that the MATLAB program managed to find and measure the extension of the complex in all images in the stack.

3

Materials and Methods

THIS CHAPTER WILL describe the chemicals used and how different solutions were prepared. It also describes the methods and how the analysis was performed.

3.1 Chemicals

The TBE buffer was prepared from 10×TBE tablets purchased from Medicago which were dissolved in milliQ water to the desired concentration of 0.5 and 0.05×TBE respectively. DNA from phage lambda (λ DNA, 48.5 kbp) was purchased from New England Biolabs and was diluted in 0.5×TBE buffer to gain proper concentrations. DNA from phage T4 GT7 (T4DNA, 166.5 kbp) was provided by Nippon Gene and purchased through Wako and was diluted in 0.5×TBE buffer to gain proper concentrations. The lipid buffer was prepared with 100 mM NaCl, 10 mM Tris base, 10 mM Boric acid and 0.225 mM EDTA at pH 8.0. DTT was used at a concentration of 50 mM , unless stated otherwise, in all TBE buffers. The inclusion of DTT in all TBE buffers is from now on no longer stated.

3.1.1 Dyes

The different dyes used in this project are presented in Table 3.1.

Table 3.1: FIS was labelled with Alexa Fluor, DNA with Cy3 and lipids in the lipid-bilayer with Rhodamine B. The reported values are from the included instruction for each dye.

Dye	Absorbance (nm)	Emission (nm)	Extinction Coefficient (M ⁻¹ cm ⁻¹)
Alexa Fluor 488	495	519	73 000
Alexa Fluor 647	650	668	270 000
Cy3(Label IT)	550	570	150 000
Rhodamine B	560	580	93 000

3.1.2 Liposome Preparation

Unlabelled lipids (POPC lipids), 25mg lipids per 1mL chloroform, were purchased from Avanti. Labelled lipids (Rhodamine tagged DHPE lipids) were purchased from Invitrogen and delivered as a powder which was dissolved as 5mg lipids per 1mL of chloroform. A 1% labelled liposome stock solution was prepared by mixing 198μL POPC stock + 10μL DHPE stock + 250μL chloroform in a round bottom flask (5mg of lipids in total). The solvent was evaporated with a rotary evaporator and then left under vacuum overnight to remove any remaining traces of solvent. The dry lipids were rehydrated with 5mL lipid buffer and vortexed to yield 1mg/mL lipid concentration. This stock solution was stored in a freezer at −20°C.

1mL of stock solution was thawed in room temperature. All extruder parts were washed with milliQ water. Filter supports were wetted with lipid buffer and placed on the internal membrane supports and the 50nm pores membrane was placed on one of the internal membrane supports and placed in the outer casing. The other internal membrane support was placed on top and the outer casing was sealed with another outer casing by hand force. 0.8mL lipid buffer was transferred through the assembled extruder 9 times by 2 syringes to clean the extruder, the buffer was then discarded. The thawed stock solution was extruded 51 times and placed in the fridge for later use in the coating of the nanofluidic chip.

3.2 Protein

The FIS protein labelled with the dyes described in Table 3.1 was kindly supplied by Prof. M. Modesti (France) (an electrophoresis gel is shown in Appendix A). The concentration was determined by a spectrometer, using the extinction coefficient of the dyes, assuming 100% labelling of the sample and 1 dye per protein, to $1\mu M$ and $2\mu M$ for FIS-488 and FIS-647 respectively. $10\mu L$ aliquots of the protein solution were stored separately in the freezer at $-80^{\circ}C$ and was thawed on ice before use and stored in the freezer between experiments.

3.3 Preparation and Coating of the Nanofluidic Chip

When preparing the nanofluidic device the chip was first mounted to the chuck by 4 screws and a metal plate. The chuck was mounted to the microscope and $20\mu L$ lipid buffer was added to one of the reservoirs. The chip was inspected with a $100\times$ oil immersed objective to visually confirm that the buffer spread by capillary forces in the chip and that no air bubbles were formed in the nanochannels. $20\mu L$ was added to the other 3 reservoirs and the formation of air bubbles in some of the reservoirs and microchannels were inevitable. The bubbles were removed by connecting the nanofluidic device to an air pump which increased the pressure to approximately $2400mbar$ in the device over night. The wetted chip connected to the chuck was then stored in the refrigerator until the time for lipid coating.

When coating the chip with a lipid-bilayer $20\mu L$ lipid buffer was removed from one reservoir and $20\mu L$ of extruded liposomes were added. Approximately $4000mbar$ of pressure was used to drive the liposomes through the microchannel where they adhere to the surface and spontaneously fuse and rupture, forming a lipid-bilayer on the surface of the channel. The opposite microchannel was coated in the same way and the lipid-bilayer from the microchannels started to enter the nanochannels. After 15min the flow direction was changed to go through the nanochannels to speed up the coating. After approximately 45min the channels were completely covered with a homogeneous emission intensity from the lipid-bilayer which was considered to have coated the chip. All reservoirs were then washed with lipid buffer 2 times and $50\mu L$ of buffer was added to all reservoirs and the pressure was lowered to $800mbar$. The buffer was then allowed to rinse the chip of all excess liposomes and all reservoirs were washed again 2 times with the desired buffer (lipid buffer for storing or TBE buffer for experiments). If the device was prepared for experiments the same day as coating, the TBE buffer was allowed to rinse the chip for approximately 1h to change the buffer in the chip from lipid buffer to the desired TBE buffer. After the experiment, the reservoirs were

washed with $50\mu L$ lipid buffer 2 times in each reservoir and the chip was rinsed with $50\mu L$ lipid buffer for 45min. The reservoirs were then washed 2 times and the nanofluidic device was stored in a refrigerator.

After storing the coated chip in the refrigerator the lipid-bilayer became damaged and holes in the coating were visible in the microscope. The lipid-bilayer was repaired by performing the same steps as for coating the chip, this repairing process took less time than the first coating (approximately 10min to reach homogeneous emission intensity).

3.4 Experiments with DNA-FIS Complexes in a Nanofluidic Device

After the nanofluidic device was prepared as described in Section 3.3 the protein was thawed on ice while the DNA was heated in a heating block at $50^{\circ}C$ for 10min, and then placed on ice. The experiment sample was then prepared by pipetting DNA with a wide pipette tip to avoid DNA damage, and mixed with the desired TBE buffer to obtain a DNA concentration of $0.8\mu M$. Protein was added to obtain the desired DNA-FIS ratio (20:1) and the solution was mixed by pipetting with a wide pipette tip gently up and down 5 times. The experiment sample was then placed in aluminium foil and allowed to form complexes for 10min in room temperature. Buffer in one reservoir of the chip was exchanged with $20\mu L$ of experimental sample which was introduced by a metal pipette tip. By applying $800mbar$ of pressure the complexes were moved into the microchannel and then introduced into the nanochannel as described in Section 2.2. Depending on the type of experiment, the complexes were then imaged by the EMCCD camera in different ways as described in Section 3.4.1-3.4.3.

3.4.1 Funnel and Straight Chip Experiments

DNA-FIS complexes were studied with different camera exposure times and the image acquisition setting was to take 200 images as fast as possible, approximately 32s. When a complex confined to the straight chip was measured several times, the complex was not moved between these measurements. The complexes studied in the funnel chip were allowed to enter the nanochannel from the wider end and were then moved to the narrower end. At least 3 measurements were made of the complexes in different confinements were each measurement consisted of 200 images.

3.4.2 Tandem and Interval Experiments

For the tandem and interval experiments the exposure time was set to $100ms$ and the image acquisition setting was to take images as fast as possible for $65s$ in the constant case. For the $1s$ interval case the exposure time was $100ms$ and the camera was instructed to take one image as fast as possible every $1s$ and to have the lights off between measurements, images were acquired for $65s$. For the $2s$ interval case, the same settings were applied except for the interval. Changing the interval times were done in the same menu in the program so it took some time to make this change but switching between interval and constant could be done instantaneously.

3.4.3 T4DNA Experiments

The camera setting for the experiments with T4DNA had the exposure time set to $100ms$ and the image acquisition setting was to take images as fast as possible for $5s$. The field of view for the camera was reduced in order to increase the imaging speed of the camera, the original field of view was 512×512 pixels and the new was set to 300×100 pixels. This resulted in approximately 10 images per second. A stopwatch was used to measure the time between measurements which were $25s$ or $50s$ intervals with 5 or 3 measurements respectively for the investigated complexes. The difference between these experiments was the number of measurements performed on the complex. The complexes measured with $25s$ intervals ran for $125s$ and complexes with $50s$ intervals ran for $115s$.

3.5 Preparation and Experiment with Label IT

The λ DNA was labelled with Cy3 using the kit Label IT following the included instructions. $0.5 \times$ TBE buffer (with no DTT) was used and the DNA concentration in the sample was $0.8\mu M$ (DNA concentration empirically determined to be suitable for the chip). The exposure time was set to $100ms$ and the image acquisition setting was to take 200 images as fast as possible, approximately 6 images per second.

3.6 Image Analysis

Image analysis was carried out using the freeware ImageJ (imagej.nih.gov) and a custom written MATLAB program (SMATool). Kymographs, where each line represents one frame in the image stack, was first constructed with ImageJ and then used by the SMATool to obtain average extensions and fluctuations for each

complex. The program analyses each line in the kymograph and fits it with a linear combination of error functions [1] which gives the position and extension of the molecule in each frame, SMATool was also used to center align the kymograph. Intensity analysis was performed with another custom made MATLAB program (Appendix C) to give the emission intensity profile for each complex as well as average emission intensity.

4

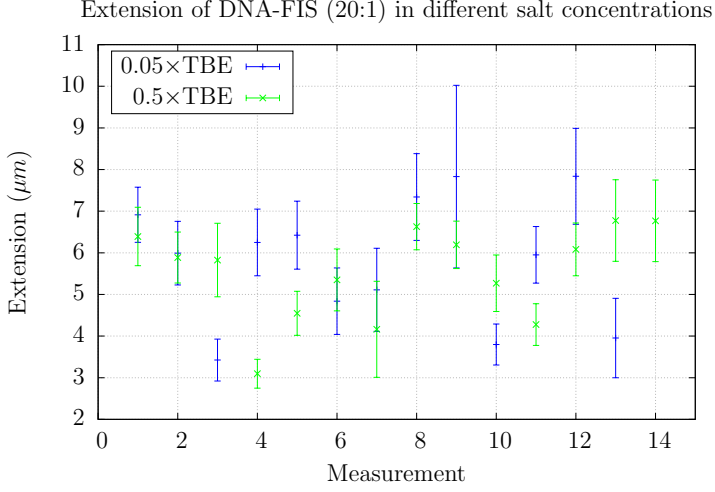
Results

THIS CHAPTER PRESENTS the results obtained from the experiments with the DNA-FIS complex investigated with a nanofluidic device and a fluorescence microscope. By using a straight chip, complexes were confined to a single confinement and the extension was studied in different salt concentrations. The extension of DNA-FIS complexes in different confinements was studied with the funnel chip. In an attempt to understand the observed drop in emission intensity for the DNA-FIS complex, a series of experiments were performed where the illumination times was varied. A candidate DNA labelling dye was also investigated for the possibility to visualize the DNA molecule and the proteins in the DNA-FIS complex simultaneously.

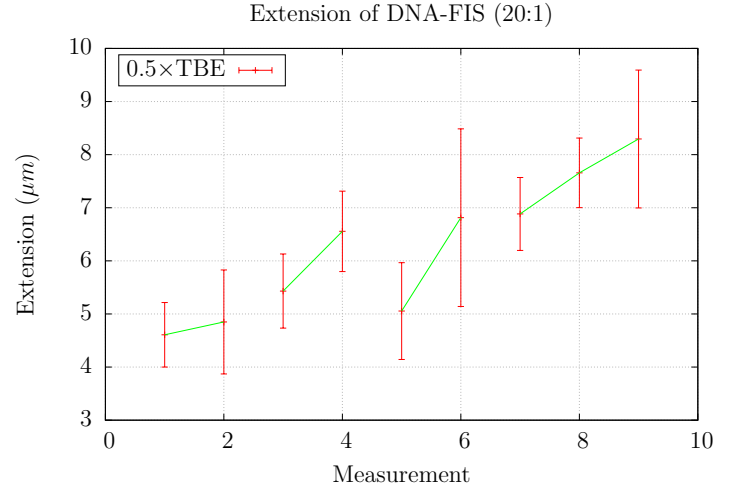
4.1 Extension of DNA-FIS Complexes in Different Salt Concentrations

By using the chip with straight nanochannels and 2 different salt concentrations (0.5 and 0.05×TBE buffer) the DNA-FIS (20:1) complex extension was studied to better understand the influence of salt concentration on the complex. Each measurement was performed during 32s. The average extension (Figure 4.1a) of the complexes was not observed to change significantly between the 2 buffer conditions. Previous studies with DNA molecules only, showed that the persistence length was inversely proportional to the ionic strength of the buffer and that the effective width varies with ionic strength [24]. This makes a DNA molecule more extended in buffers with lower salt concentrations. The DNA-FIS complex however did not become more extended in the lower salt concentration which would suggest that the binding of FIS changed the physical properties of DNA. Performing 2 or 3

consecutive measurements on 4 complexes in $0.5\times$ TBE buffer (Figure 4.1b) showed that the complexes got more extended in later measurements which could be due to dissociation of proteins or that the complex needs a significant amount of time to reach extension equilibrium. Measurements were performed during approximately¹ 32^2s and the next measurement was made within $20s$.



(a)



(b)

Figure 4.1: (a) The average extension with standard deviation as errorbars of complexes in 0.05 and $0.5\times$ TBE buffer, where the extension of the complexes are similar in the 2 buffers. (b) The average extension of 4 complexes when measured at 2 or 3 consecutive times indicated with connecting lines. The average extension becomes larger with time.

¹The camera takes 200 images during $32s \pm 1$ second.

²Measurement 1 and 2 was made during $42s$ then, the exposure time was changed from $150ms$ to $100ms$

4.1.1 Sequence Specific Binding of FIS

When investigating the DNA-FIS complex in different salt concentrations, it was observed that different types of emission patterns (Figure 4.2) on the DNA-FIS complex were present when confined in the straight chip. These emission patterns indicated sequence specific binding to GC-rich regions compared to AT and that the binding was heterogeneous, resulting in a variety of complexes with different DNA-FIS compositions when mixed 20:1. In the $0.5\times$ TBE buffer, 30 out of 32 complexes showed patterns (Striped 2x + Striped 3x + Transition + Inexplicit) while in the $0.05\times$ TBE buffer, only 16 out of 40 complexes showed patterns. It might be that the lower salt concentration promotes more FIS proteins to bind to DNA and less patterns were observed, or that the lower salt concentration makes the FIS protein bind DNA more tightly and less protein dissociates when confined to the nanochannel. Another possibility is that the lower salt concentration changes the specificity of the FIS protein for GC- and AT-rich regions and that the binding distribution becomes more homogeneous.

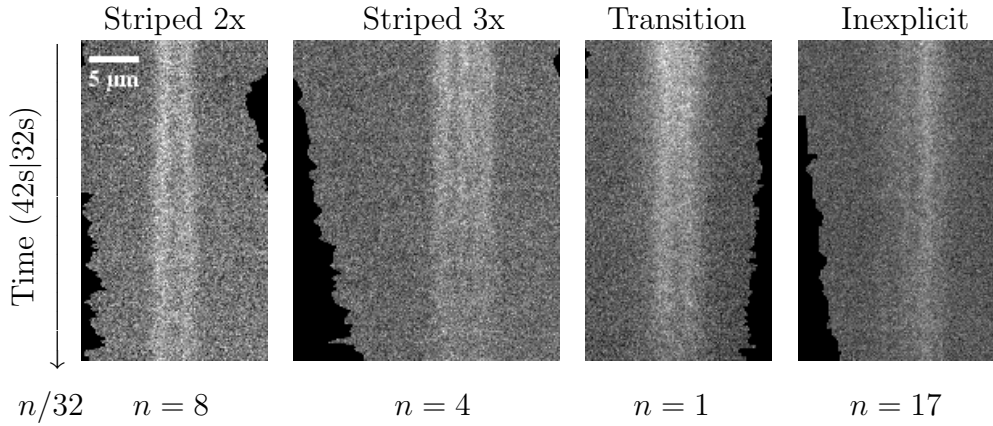


Figure 4.2: 4 different center aligned kymographs from 200 images showing different types of pattern on λ DNA in $0.5\times$ TBE buffer. Due to different exposure times ($150ms$ and $100ms$) the duration of the striped 2x kymograph was measured during $42s$ and all the others during $32s$. Out of 32 complexes, 8 was striped 2x, 4 was striped 3x, 1 transitioned from no pattern into striped 2x and 17 showed some kind of pattern that did not fit the striped 2x or 3x pattern, the remaining 2 complexes showed no pattern. The scale bar shows the length of $5\mu m$.

The average emission intensity profile along the Striped 3x complex (Figure 4.3) showed a pattern with one large and one smaller drop which is similar to profiles reported previously for GC/AT mapping of λ DNA [3]. The intensity profile along the DNA-FIS complex corresponds well with GC rich regions where the intensity is higher and lower for AT rich regions. This indicates that the FIS protein has a higher affinity for GC rich regions compared to AT as previously suggested [8].

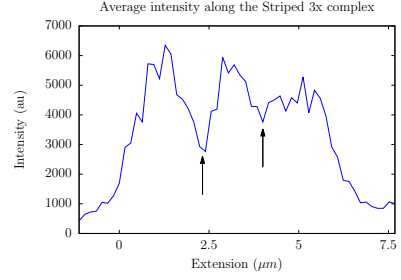


Figure 4.3: Striped 3x complex average intensity profile.

4.2 Extension of DNA-FIS Complexes in Different Confinements

To investigate how the extension of the λ DNA-FIS (20:1) complex varies with confinement, a funnel chip ($800 \times 140 \text{ nm}^2 \rightarrow 100 \times 140 \text{ nm}^2$) with $0.5 \times$ TBE buffer was used. It was possible to measure the first complexes several times at different confinements (Figure 4.4a) before the intensity became too faint. It is unclear whether the decrease in intensity over time was due to bleaching of the dye or if the FIS protein dissociated from the DNA. The increased extension of the complex (similar to the complex in Figure 4.1b) when returned to a previous confinement suggested that some of the proteins dissociated. The extension was fitted to the rewritten (Appendix B) deGennes theory equation (Section 2.6):

$$\frac{r}{L} = \left(\frac{\omega_{eff} P}{D_{AV}^2} \right)^{\frac{1}{3}} \Rightarrow f(x) = c(x140)^{-\alpha} \quad (4.1)$$

where $f(x)$ is the measured extension as a function of confinement x , c is $L(\omega_{eff} P)^{\frac{1}{3}}$ and α is theoretically $\frac{1}{3}$. L is the contour length, ω_{eff} is the effective width, P is the persistence length and $x140$ is the cross section area of the nanochannel in the funnel chip. The complex shown in Figure 4.4 has an α value of 0.36 which is close to deGennes' predicted 0.33. However, the fitted c and α values for each complex (Figure 4.4b) showed an exponential relationship and not the predicted $\alpha = 0.33$. deGennes theory could therefore not be used to describe the behaviour of all the complexes in the funnel chip.

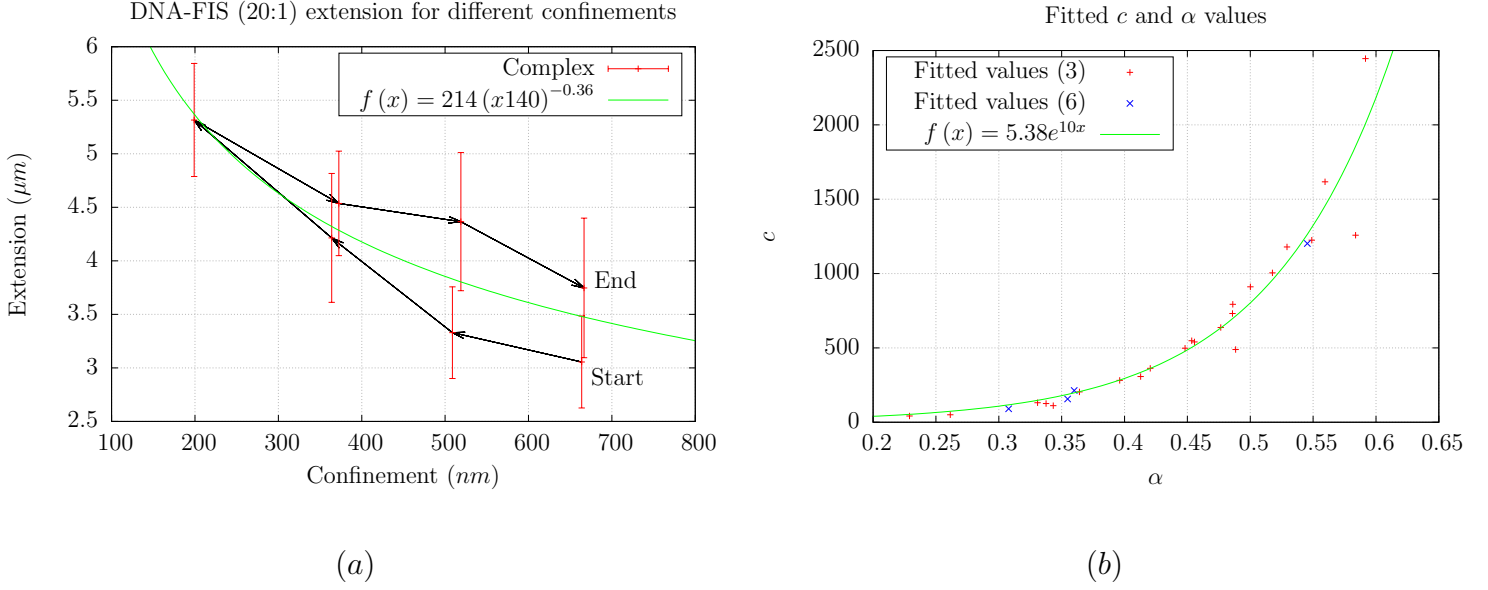


Figure 4.4: (a) The extension of one complex when confined in different confinements and how extension increases in smaller confinements and when the complex was moved back for a second measurement, standard deviations are shown as errorbars. Start and End indicates first and last measurement and black arrows the order of measurement. The solid green line shows the fitted Equation 4.1 with $c = 214$ and $\alpha = 0.36$. (b) The relationship between the fitted c and α values for 27 different complexes. Red cross hair are values fitted to 3 measurements and blue cross are values fitted to 5 or 7 measurements.

The emission intensity of all λ DNA-FIS complexes became very weak after the 4 first complexes had been measured. It was only possible to measure the remaining complexes 3 times before the emission intensity was too similar to the background. The fitted values are thus somewhat unreliable since only 3 points were used to make the fit for most of the complexes. Nevertheless, it still shows the exponential relationship between the c and α value, but errorbars are omitted since they would indicate a good fit. The extension of the complexes (Figure 4.5) showed a large distribution when confined to similar confinements and became more extended in smaller confinements. The large distribution of different extensions could be due to heterogeneous binding of the protein which would form some complexes with higher FIS concentrations and other complexes with lower FIS concentrations, thus different degrees of compaction.

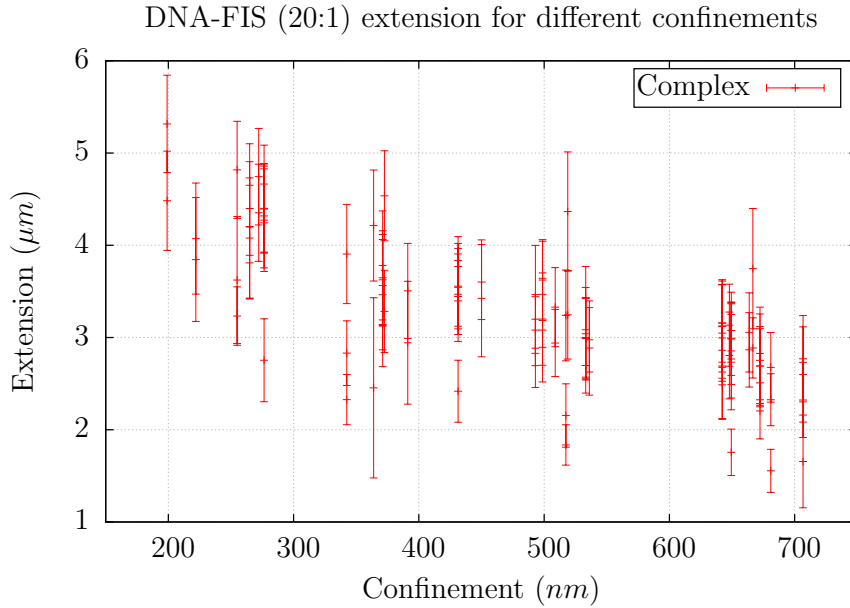


Figure 4.5: The extension of 27 different complexes measured in at least 3 different confinements. The complexes become more extended in smaller confinements but it is not clear how much more extended the complex becomes since the distribution of different extensions are wide spread.

4.3 The Intensity Problem, Bleaching and/or Dissociation?

During the initial investigations of the DNA-FIS complex it was observed that the emission intensity decreased faster than expected. It was not clear if this was due to bleaching of the dye or if the protein dissociated from the complex when confined in the nanofluidic device. In order to investigate the influence of bleaching of the DNA-FIS complex, a series of tandem experiments were carried out in a straight chip with $0.05 \times \text{TBE}$. First, measurements were done in intervals of 1s where the lamp was turned off between measurements. Then, the constant condition was applied and the lamp was turned on for the whole duration of the experiment (Figure 4.6a), each part took 65s. It was expected that the rate of intensity decrease would be faster under the constant condition when the lamp was constantly on compared to intervals if bleaching was a large contributor to the intensity drop. However, the rate of intensity decrease was in some cases the other way around (Figure 4.6b). The sometimes quick intensity drop rate

posed a problem to get reliable intensity measurements since the intensity might have already reached the lowest value when the signal to noise ratio was to low (approximately around $500au$ to $1000au$) when the constant condition was applied. Attempts were made to first apply the constant condition and then the interval but the complexes became to faint for analysis to be successful.

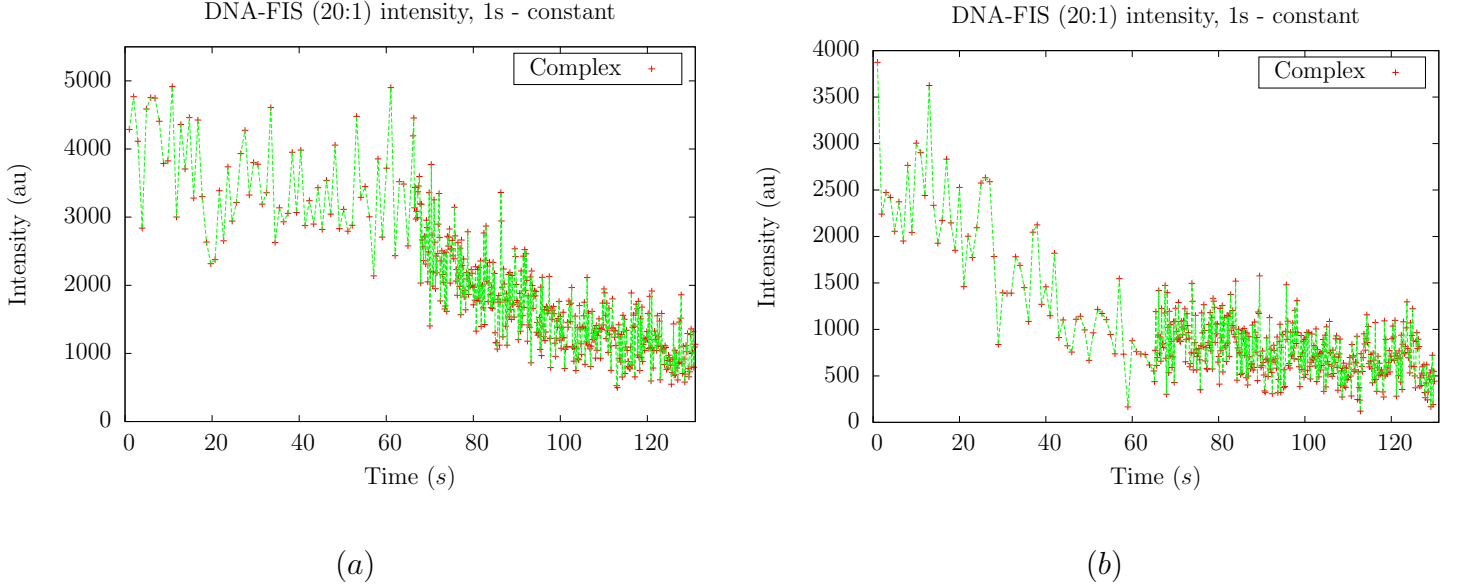


Figure 4.6: λ DNA-FIS (20:1) complexes in $0.05\times$ TBE buffer (a) a tandem experiment where the measurements for the first 65s were done in 1s intervals, then for another 65s measurements was made continuously. This illustrates that the intensity drop was highly dependent on the amount of light used. (b) shows another complex where the intensity drop rate was faster in the interval case compared to the constant.

The intensity drop rate was investigated further by studying several complexes with measurements in 0, 1 and 2s intervals (Figure 4.7a). The intensity drop rate varied between different complexes that were measured under the same conditions and there was no clear trend between the start intensity (m) and the rate of decreased intensity (k) for the 0s and 1s intervals. The complexes measured in 2s intervals showed a trend where the higher intensity tended to give a higher rate of intensity drop. In addition, the interval experiments were performed during 65s or 130s, the number of complexes collected for each time duration was roughly evenly divided between the different durations. When performing the image analysis of the 130s duration experiments, tracing of the complexes failed in some cases due to a low intensity towards the end of the experiment and these could therefore not be

included in the results. The 0s experiments included 13|0 (65s|130s) complexes, 1s included 7|6 complexes, 2s included 1|5 complexes (here, more 130s experiments were performed because the complex was observed to have a high intensity after 130s).

A tandem experiment where a 2s interval and then a 1s interval was used (Figure 4.7b) showed that there was a significant change in intensity between the measurements. Approximately 1min time delay between the 2 intervals was spent to adjust the microscope setting to change the imaging interval to 1s. During this time the intensity of the complex dropped from about 3000au to 1500au which could indicate dissociation of the DNA-FIS complex since the sample was not illuminated during this time.

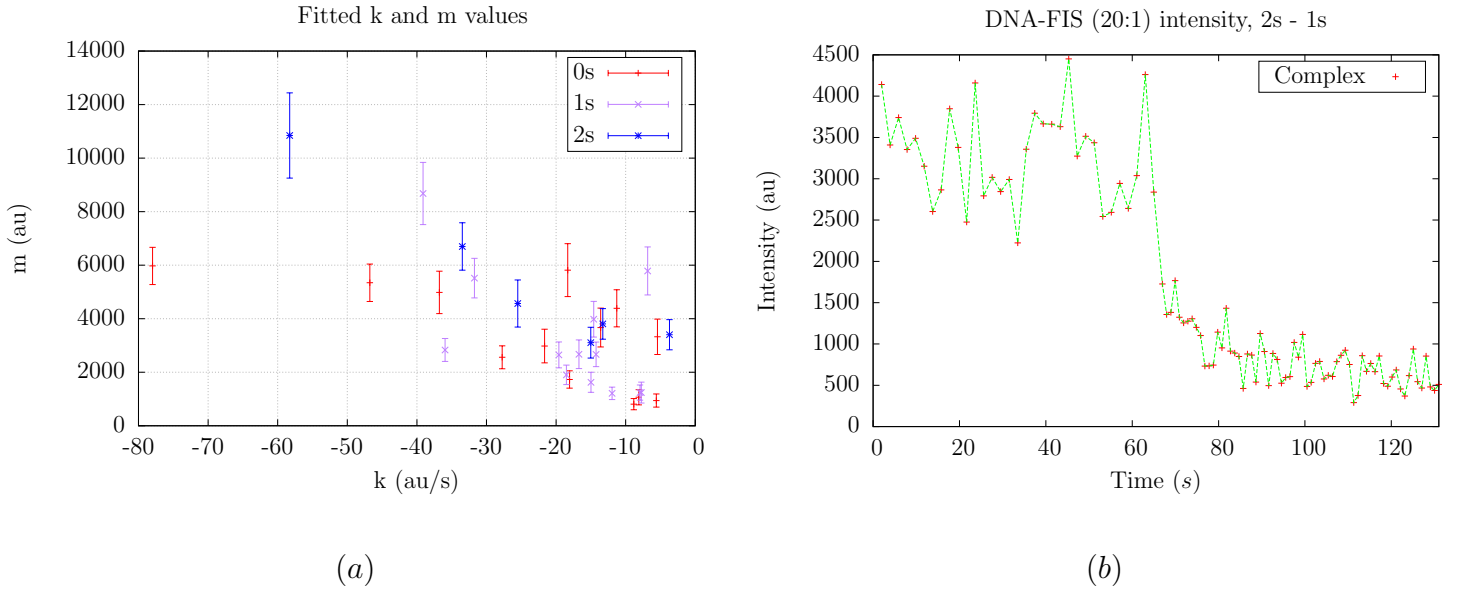


Figure 4.7: λ DNA-FIS (20:1) complexes in 0.05 \times TBE buffer (a) each complex fitted k and m value to $f(x) = kx + m$ in the 0, 1 and 2s interval experiments. There was no clear trend for the 0s and 1s complexes and the 2s interval complexes showed a trend where a higher intensity corresponds to a higher intensity drop rate. (b) shows a tandem experiment with approximately 1min time delay between the experiments, the intensity drop between the experiments could indicate that some FIS proteins dissociated from the DNA-FIS complex since the illumination of the sample during that time was turned off.

In order to investigate the suspected dissociation, an experiment where measurements were made for 5s followed by 50s without illumination, was repeated 2 times and ended with a 5s measurement for 12 complexes (Figure 4.8). In

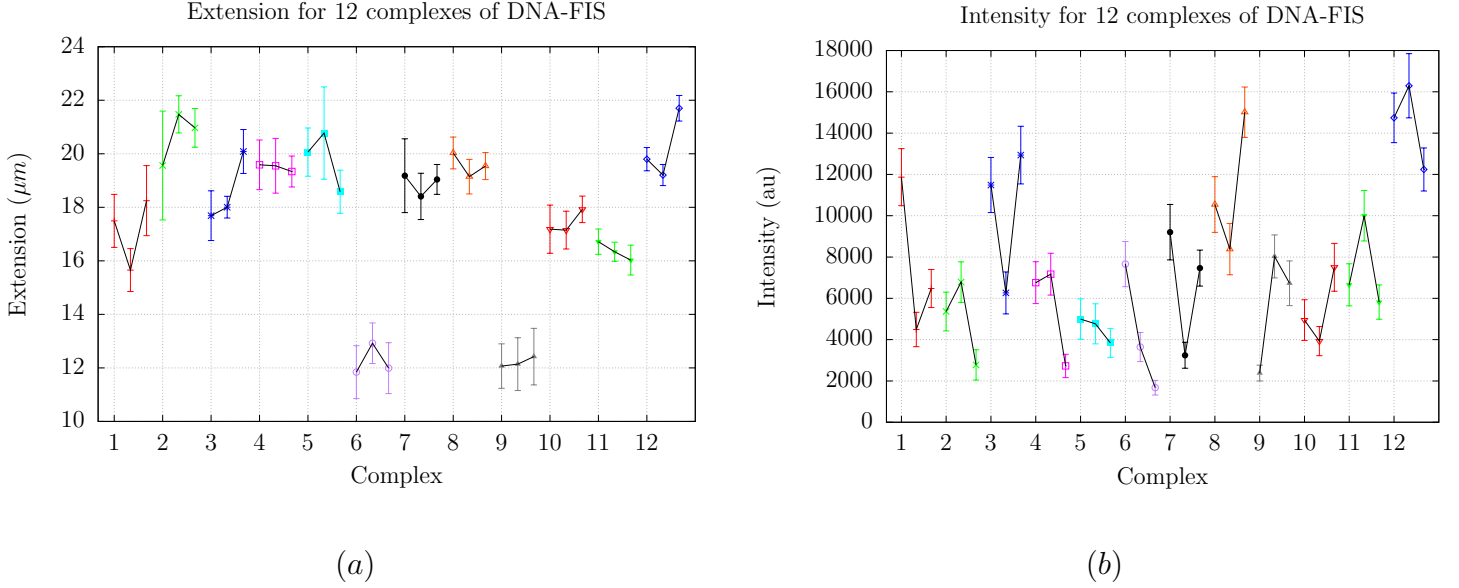


Figure 4.8: T4DNA-FIS (20:1) complexes in $0.5\times\text{TBE} + \text{DTT}$ ($0.1M$) buffer with different symbols and colors measured for 5s at 3 different times (ending at 5, 55 and 110s). The average extension (a) with standard deviation as errorbars of each complex are shown and there was no clear trend of elongation or retraction. The average intensity (b) with standard deviation as errorbars for each complex is shown in corresponding symbols and colors as for the extension. No clear relationship between the extension and the intensity was found.

these experiments T4DNA was used and the DNA-FIS complex ratio was kept at 20:1. T4DNA contains approximately 3.5 times more base pairs than λ DNA which means that more DNA-FIS associations per complex could be studied. To minimize the effects of bleaching, twice the DTT concentration compared to the standard condition was used. The average extension of the complex (Figure 4.8a) did not show a clear trend of becoming more or less extended with time. The average extension of all complexes were under $22\mu\text{m}$ which seems reasonable compared to λ DNA which showed extensions under approximately $6.5\mu\text{m}$ in $0.5\times\text{TBE}$ buffer (Figure 4.1a). This was to be expected since the contour length of T4DNA is approximately 3.5 times larger than that of λ DNA which would result in a 3.5 times larger extension of the complex. The less extended complexes at $12\mu\text{m}$ were probably fragmented complexes. The intensity of some complexes (Figure 4.8b) changed in unexpected ways where the intensity could be higher at the first and last measurement but significantly lower in the middle. The intensity of the complexes could not be used to determine if there was any dissociation of the protein. No correlation between the average extension and the average intensity of the complex

at different times was detected.

The same experimental setup was used once more with the only difference being the number of measurements performed on the complex during 120s (Figure 4.9). These 3 complexes showed a similar behaviour as in the previous experiment with fewer measurements. The higher resolution in this case (5 5s measurements during 120s compared to 3 5s measurements during 110s) showed that the extension is rather constant, although small fluctuations occur, and that a systematic drop in intensity could not be seen. No dissociation of the FIS protein could therefore be confirmed. Compared to the intensity drop when constantly illuminated, these results show that when shorter illumination times are used the intensity does not drop significantly which would indicate that bleaching is the largest factor for the intensity drop.

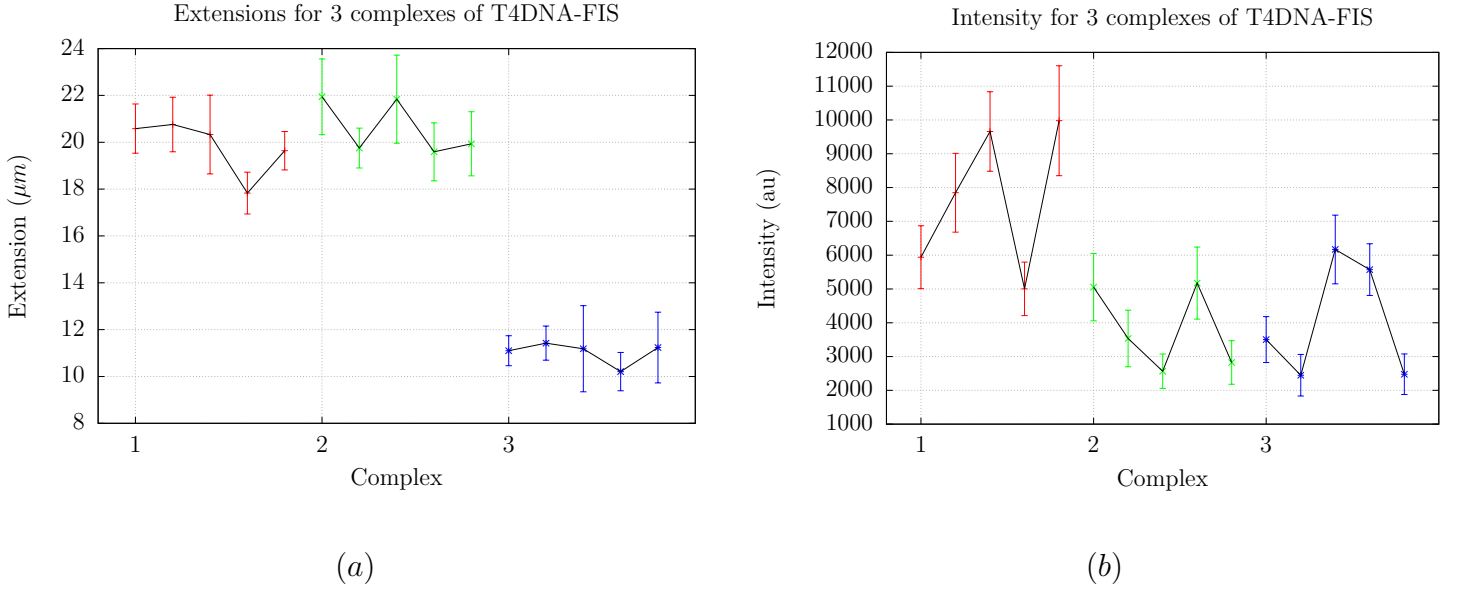


Figure 4.9: T4DNA-FIS (20:1) complexes in $0.5 \times \text{TBE} + \text{DTT}$ ($0.1M$) with different symbols and colors measured for 5s at 5 different times (ending at 5, 30, 60, 90 and 120s). The average extension (a) with standard deviation as errorbars of each complex shows no clear trend of elongation or contraction. The average intensity (b) with standard deviation as errorbars of each complex is shown in corresponding symbols and colors as for the extension. No clear relationship between the extension and the intensity was found.

4.4 Label IT to Covalently Label DNA

It would be possible to investigate how much of the DNA molecule that was covered with proteins if both DNA and FIS could be visualized separately. The labelled DNA could potentially be used in future studies of other DNA-protein complexes. To visualize DNA in a nanochannel a dye molecule needs to be attached to it. It was desired that the dye had a high emission intensity and that it affected the physical properties of DNA as little as possible. Label IT is a commercial kit that offers a fast and easy labelling process of DNA where a dye molecule becomes covalently bond to the DNA backbone.

The straight chip with $0.5\times$ TBE buffer was used to investigate the average extension of the Label IT labelled λ DNA (Figure 4.10). The extension of λ DNA with $0.5\times$ TBE buffer in non-coated straight nanochannels were previously determined to be $7.8\mu m$ (unpublished by Lena Nyberg). The extensions close to $9\mu m$ showed here were surprising but might be due to the lipid-bilayer or the way the kit labels the DNA. There were no problems with bleaching when studying the dyed DNA but since the results showed a partially labelled or damaged DNA molecule, it was not used further in this project.

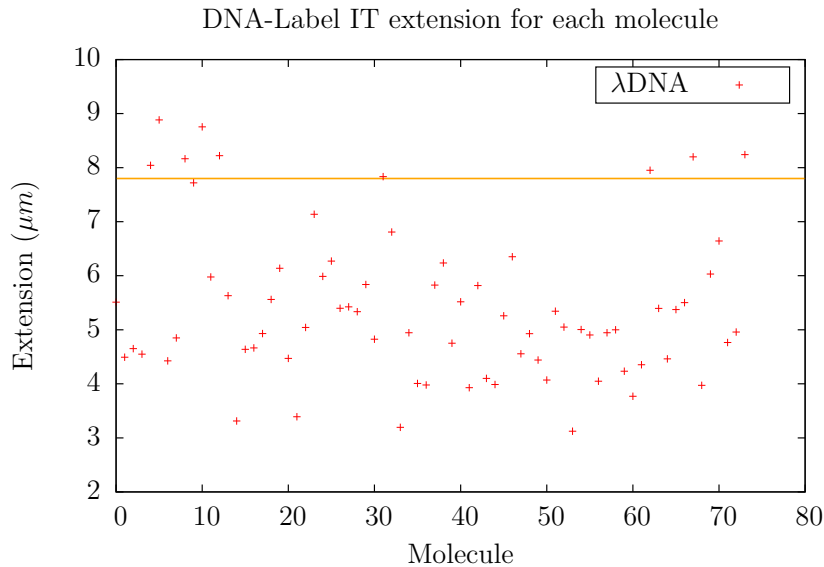


Figure 4.10: The average extension of DNA labelled with the kit Label IT from Mirus. The wide distribution of extensions could be due to damages to the DNA in the labelling process. The orange line is the longest expected extension.

5

Discussion

THIS CHAPTER DISCUSSES the results obtained from the experiments with DNA-FIS complexes as well as the candidate DNA labelling dye. It also discusses experiments that can be performed in order to validate some of the preliminary results obtained in this initial study.

5.1 Are the DNA-FIS Complexes Affected by Different Salt Concentrations?

The extension of the DNA-FIS complex was not seen to be affected by the tested salt concentrations. Previous studies have shown that the persistence length of a DNA molecule is inversely proportional to the ionic strength of the buffer and that the effective width varies with ionic strength [24]. This makes the DNA molecule more extended in buffers with lower salt concentrations. The DNA-FIS complex is probably less affected by the ionic strength of the buffer solution since FIS lowers the overall negative charge of the DNA molecule when it binds. However, the salt concentration was observed to influence the FIS binding pattern on the DNA molecule. This could indicate that the lower salt concentration allowed for more FIS to bind, which would make the complex less extended since FIS packages the DNA molecule, but the DNA molecule becomes more extended due to the lower ionic strength in the buffer solution. These 2 effects might cancel each other out and leave a small net extension change.

5.2 Is a Sequence Specific Binding Distribution of FIS Detectable?

When confining the DNA-FIS (20:1) complex to the $100 \times 150 \text{ nm}^2$ chip, different patterns were observed. FIS has previously been demonstrated to have a higher affinity to GC-rich regions compared to AT [8]. When comparing the pattern of FIS binding to λ DNA and optically mapped λ DNA [3], the intensity profiles for the Striped 3x complexes (Figure 4.3) were very similar to the mapped profile. This demonstrates that sequence specific binding of the protein can be visualized and investigated. The different patterns were probably due to different amounts of bound FIS which likely affects the physical properties of the complex. It would be possible to use a nanofluidic device to investigate each complex type further to better understand how the physical properties changes between different types of DNA-FIS complexes.

5.3 Can the Extension of a DNA-FIS Complex be Investigated in Different Confinements?

The results from the λ DNA-FIS complexes in the funnel chip showed that it was possible to investigate the extension of these complexes in different confinements. However, there was a fast decrease in emission intensity from the complexes which resulted in that only measurements at 3 different confinements were possible before the complexes became too faint for further imaging. In order to make reliable model fits to the measurements it is required that more measurements are made per complex. Therefore it is important to use a dye that is resistant to bleaching to enable more measurements. With that said, the complexes investigated showed an exponential relationship between the fitted c and α value. From the rewritten deGennes equation (Equation 4.1) it was expected that complexes with $\alpha = 1/3$ would behave like a series of connected blobs. A previous study of DNA stained with YOYO-1 (10:1) confined in different confinements fitted to $r = D_{AV}^\alpha$ gave $\alpha = 0.85$ [25]. The transition between the deGennes and the Odijk regimes is not that well understood [22] and how the persistence length and the effective width (Section 2.6 for DNA with no FIS bound) are affected when FIS binds is not known. One could argue that the persistence length should decrease when FIS binds because it bends the DNA molecule and that the effective width of DNA should decrease when FIS binds since it lowers the overall negative charge of the DNA molecule, all of which directed to compact DNA in the nucleoid. However, the effective width of the complex might increase when the protein is added to the DNA molecule. Depending on how much FIS that binds the DNA molecule,

the contribution of each factor (ω_{eff} and P) to the product c may change. One explanation of the relationship between the c and α values in Figure 4.4b would be that for smaller α values, the complex behaves as a series of blobs described by deGennes theory. For larger α values the complex behaves more like DNA stained with YOYO-1 where the amount of base pairs per blob is too small for it to be considered a blob and the complex forms hairpin like structures. In complexes with more FIS bound, DNA is expected to be more compacted and if the argument about how FIS decreases persistence length and effective width are correct, it would mean that complexes with a high FIS content would behave more like blobs. One way of investigating this in the nanofluidic device would be to add FIS in great abundance, for example DNA-FIS (5:2), and investigate if $\alpha \approx 0.33$ for all complexes in the funnel chip.

5.4 Is the Intensity Drop Due to Bleaching and/or Dissociation of FIS?

When investigating the λ DNA-FIS complex it was unclear if there was any dissociation of FIS. The 2s interval experiment showed that complexes had a high intensity at the end of the 65s measurements and that more measurements could be performed during 130s. Comparing the amounts of possible 130s measurements between 0s and 2s intervals showed that bleaching was prevalent. The investigated T4DNA-FIS complexes did not show a trend where the complex became more or less extended with time and the intensity did not show a fast drop when low amounts of illumination was applied. This suggested that FIS stayed bound to the DNA molecule in the nanochannel and that bleaching was probably the reason for the intensity drop. The observed extension increase of λ DNA-FIS complexes with time was possibly due to a slow unpacking of the DNA-FIS complex when extended in the nanochannels, but dissociation of FIS could not be ruled out. Both FIS-488 and FIS-647 were tested in this project but both dyes showed the same problem with decreasing emission intensity. It would be easy to test if the Alexa Fluor dyes were the problem by simply testing another dye for example ATTO-488.

5.5 Can Label IT be Used to Covalently Label DNA?

It would be possible to investigate how much of the DNA molecule that was covered with proteins if both DNA and FIS could be visualized separately. After the dye was covalently bound to the DNA molecule using the Label IT kit, it was observed that there was a wide distribution of different extensions of dye-DNA molecules in the nanochannels. It was argued that this distribution was because the DNA got damaged in the labelling process and that Label IT could therefore not be used to covalently label DNA to be used in nanochannel studies. Therefore, no investigation was made where the DNA was labelled and then mixed with FIS. This initial study of Label IT was not thorough enough to completely rule out Label IT as a candidate to covalently label DNA for nanofluidic applications. In order to investigate if the DNA molecule gets damaged in the labelling process a gel electrophoresis with DNA from the different steps could be analysed. This includes λ DNA before labelling, dye- λ DNA after the labelling process and a sample of dye- λ DNA after ejection from the metal pipette tip. This was not performed and therefore it was simply stated that Label IT was not further used in this study to label DNA.

One benefit of not using any dye to stain the DNA molecules in this study was that the extension of the complexes observed here could be used as a reference when a suitable DNA dye is found. The future experiments with dye-DNA-FIS complexes could then be compared to the extensions of the complexes in this study to determine if the dye affect the DNA-FIS complex.

The influence the dye molecule attached to FIS had on the protein structure and function was not investigated in this study. Since the protein was observed to bind the DNA molecule it was assumed that the dye's influence on the protein was low.

6

Conclusions

THE INITIAL STUDIES performed in this thesis have provided some new insights to the DNA-FIS interaction in nanofluidic devices. More studies needs to be performed to validate the interactions between DNA and FIS in nanochannels. The insights gained from this study are not limited to the DNA-FIS interaction but could be applied to other DNA-protein studies.

- Experiments at different salt concentrations showed that the binding distribution of FIS was affected while the extension of the DNA-FIS complex was not. This shows that the protein changed the physical properties of the DNA molecule which could be detected in the nanofluidic device. Sequence specific binding of GC-rich regions of FIS were detected on λ DNA and the lower salt concentration ($0.05\times$ TBE) yielded less complexes with patterns.
- It was possible to investigate the DNA-FIS complex at different confinements, but the emission intensity dropped faster then expected which made it difficult to study the complex for longer time periods. For future studies, the dye could be exchanged with ATTO-488 to decrease the bleaching which would make more measurements possible.
- If the intensity drop was due to bleaching and/or dissociation of FIS was unclear when illuminating the complexes for longer times. When lowering the amount of illumination it was observed that the intensity was higher for longer times and did not show a systematic decrease. FIS dissociation could not be confirmed when using shorter illumination. The drop in intensity was thus probably mainly due to bleaching of the dye.
- Staining DNA with the Label IT kit was not suitable in this study since it

seemed to damaged the DNA in the labelling process. However, the emission intensity and resistance to bleaching was satisfactory.

Bibliography

- [1] J. O. Tegenfeldt, C. Prinz, H. Cao, S. Chou, W. W. Reisner, R. Riehn, Y. M. Wang, E. C. Cox, J. C. Sturm, P. Silberzan, R. H. Austin, The dynamics of genomic-length DNA molecules in 100-nm channels, *Proceedings of the National Academy of Sciences of the United States of America* 101 (30) (2004) 10979–83.
- [2] F. Persson, J. O. Tegenfeldt, DNA in nanochannels—directly visualizing genomic information, *Chemical Society Reviews* 39 (3) (2010) 985–99.
- [3] L. K. Nyberg, F. Persson, J. Berg, J. Bergström, E. Fransson, L. Olsson, M. Persson, A. Stålnacke, J. Wigenius, J. O. Tegenfeldt, F. Westerlund, A single-step competitive binding assay for mapping of single DNA molecules, *Biochemical and Biophysical Research Communications* 417 (1) (2012) 404–408.
- [4] B. Alberts, A. Johnson, J. Lewis, M. Raff, K. Roberts, P. Walter, *Molecular Biology of the Cell* - fifth edition, Garland Science.
- [5] R. Marie, A. Kristensen, Nanofluidic devices towards single DNA molecule sequence mapping, *Journal of Biophotonics*.
- [6] F. Persson, J. Fritzsche, K. U. Mir, M. Modesti, F. Westerlund, J. O. Tegenfeldt, Lipid-based passivation in nanofluidics, *Nano Letter* 12 (5) (2012) 2260–5.
- [7] Y. M. Wang, J. O. Tegenfeldt, W. Reisner, R. Riehn, X. J. Guan, L. Guo, I. Golding, E. C. Cox, J. Sturm, R. H. Austin, Single-molecule studies of repressor-DNA interactions show long-range interactions, *Proceedings of the National Academy of Sciences of the United States of America* 102 (28) (2005) 9796–801.

- [8] C. Kahramanoglou, A. S. Seshasayee, A. I. Prieto, D. Ibberson, S. Schmidt, J. Zimmermann, V. Benes, G. M. Fraser, N. M. Luscombe, Direct and indirect effects of H-NS and Fis on global gene expression control in *Escherichia coli*, *Nucleic Acids Research* 39 (6) (2011) 2073–91.
- [9] P. Atkins, J. de Paula, R. Friedman, *Quanta, Matter, and Change - A molecular approach to physical chemistry*, Oxford university press, 2009.
- [10] Fluorescence, <http://en.wikipedia.org/> (November 2012).
- [11] Fluorescence microscope, <http://en.wikipedia.org/> (November 2012).
- [12] DNA, <http://en.wikipedia.org/> (May 2013).
- [13] Central dogma of molecular biology, <http://en.wikipedia.org/> (May 2013).
- [14] Translation (biology), <http://en.wikipedia.org/> (June 2013).
- [15] T. Ali Azam, A. Iwata, A. Nishimura, S. Ueda, A. Ishihama, Growth phase-dependent variation in protein composition of the *Escherichia coli* nucleoid, *Journal of Bacteriology* 181 (20) (1999) 6361–70.
- [16] D. Kostrewa, J. Granzin, D. Stock, H. W. Choe, J. Labahn, W. Saenger, Crystal structure of the factor for inversion stimulation FIS at 2.0 Å resolution, *Journal of Molecular Biology* 226 (1) (1992) 209–26.
- [17] D. Kostrewa, J. Granzin, C. Koch, H. W. Choe, S. Raghunathan, W. Wolf, J. Labahn, R. Kahmann, W. Saenger, Three-dimensional structure of the *E. coli* DNA-binding protein FIS, *Nature* 349 (6305) (1991) 178–80.
- [18] H. S. Yuan, S. E. Finkel, J. A. Feng, M. Kaczor-Grzeskowiak, R. C. Johnson, R. E. Dickerson, The molecular structure of wild-type and a mutant Fis protein: relationship between mutational changes and recombinational enhancer function or DNA binding, *Proceedings of the National Academy of Sciences United States of America* 88 (21) (1991) 9558–62.
- [19] D. Skoko, D. Yoo, H. Bai, B. Schnurr, J. Yan, S. M. McLeod, J. F. Marko, R. C. Johnson, Mechanism of chromosome compaction and looping by the *Escherichia coli* nucleoid protein Fis, *Journal of Molecular Biology* 364 (4) (2006) 777–98.
- [20] D. Skoko, J. Yan, R. C. Johnson, J. F. Marko, Low-force DNA condensation and discontinuous high-force decondensation reveal a loop-stabilizing function of the protein Fis, *Physical Review Letters* 95 (20) (2005) 208101.

- [21] T. W. Burkhardt, Y. Yang, G. Gompper, Fluctuations of a long, semiflexible polymer in a narrow channel, *Physical Review* 82 (2010) 041801.
- [22] E. Werner, F. Persson, F. Westerlund, J. O. Tegenfeldt, B. Mehlig, Orientational correlations in confined DNA, *Physical Review E* 86 (4 Pt 1) (2012) 041802.
- [23] W. Reisner, K. J. Morton, R. Riehn, Y. M. Wang, Z. Yu, M. Rosen, J. C. Sturm, S. Y. Chou, E. Frey, R. H. Austin, Statics and dynamics of single DNA molecules confined in nanochannels, *Physical Review Letter* 94 (19) (2005) 196101.
- [24] N. Douville, D. Huh, S. Takayama, DNA linearization through confinement in nanofluidic channels, *Analytical and Bioanalytical Chemistry* 391 (7) (2008) 2395–409.
- [25] F. Persson, P. Utko, W. Reisner, N. B. Larsen, A. Kristensen, Confinement spectroscopy: probing single DNA molecules with tapered nanochannels, *Nano Letter* 9 (4) (2009) 1382–5.

Appendices

A

Protein Purity

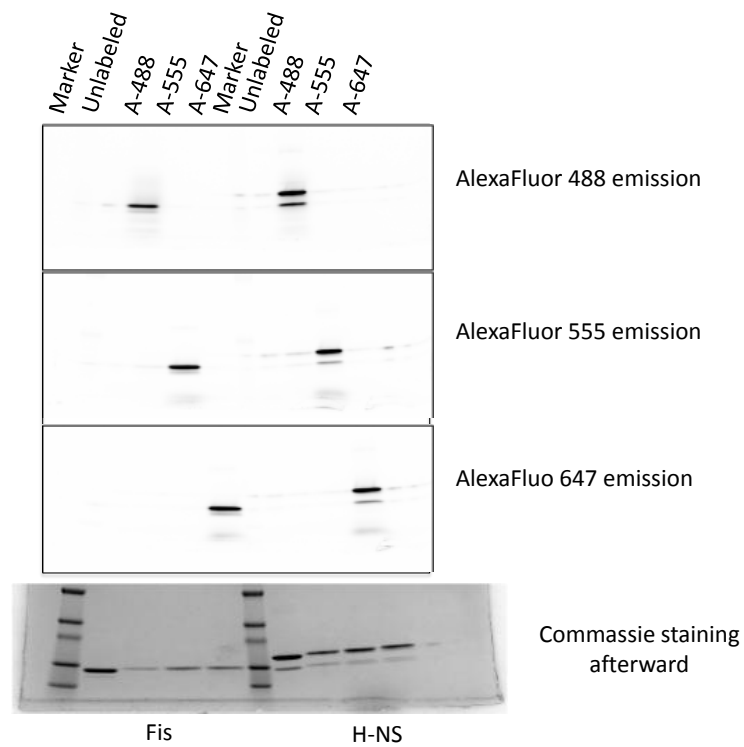


Figure A.1: Illustrates the electrophoresis gel supplied by Prof. M. Modesti (France), the top part shows the Alexa Fluor 488, 555 and 647 emissions for Fis (left) and H-NS (right) respectively. The bottom part shows the comassie staining afterwards. Only Fis was investigated in this study.

B

Rewritten deGennes Equation

The deGennes equation can be written as:

$$\frac{r}{L} = \left(\frac{\omega_{eff} P}{D_{AV}^2} \right)^{\frac{1}{3}} \quad (\text{B.1})$$

where r is the observed length, L is the contour length, ω_{eff} is the effective width, P is the persistence length and D_{AV}^2 is the cross section area of the nanochannel. Since the channel width in the funnel chips changes we denote it with x , the depth of the nanochannel is constant at $140nm$, thus $D_{AV}^2 = x140$. The deGennes equation can be rewritten as the measured extension as a function of x :

$$r(x) = L (\omega_{eff} P)^{\frac{1}{3}} (x140)^{-\frac{1}{3}} \quad (\text{B.2})$$

and by using $c = L (\omega_{eff} P)^{\frac{1}{3}}$ and $-\alpha = -\frac{1}{3}$ the equation can be written as:

$$f(x) = c (x140)^{-\alpha} \quad (\text{B.3})$$

which is used to investigate if the extension of the DNA-FIS complex follow deGennes theory in the funnel chip.

C

MATLAB Intensity Profile Code

```
% Reads multiple .tif center align kymographs
% Calculates the integrated intensity with a cut off value for each frame.
% Then calculates the intensity mean and std of each image.

function [raw] = Intensity_batch(varargin)

if nargin == 0;
[filename, pathname] = uigetfile({'*.tif'}, 'Select centerlined kymograph
                                files', 'MultiSelect', 'on');

switch iscell(filename)
    case 1
        if cellfun('isempty', filename)
            disp('Error! No (or wrong) file selected!')
            return
        end
    case 0
        disp('Batch means that you should choose MULTIPLE files.')
        return
end
else
    fil = fopen(varargin{1});
    filename = textscan(fil, '%s', 'Delimiter', '\n');
    filename = filename{1};
    pathname = pwd;
end

raw = []; Int_avg = []; Int_std = [];
```

APPENDIX C. MATLAB INTENSITY PROFILE CODE

```
for fileNum = 1:length(filename)
    full_filename = [pathname '/' filename{fileNum}];
    data = imread(full_filename);
    dataT = double(data)';

    % With (W) cut off (c)
    c = mean(data(1,1:10)) + std(double(data(1,1:10)));
    dataT = dataT - c;
    dataT(dataT<0)=0;
    W = trapz(dataT);

    % Calculate average intensity
    % And standard deviation
    raw = [raw, W];
    avInt = mean(W);
    stdInt = std(W);
    Int_avg = [Int_avg, avInt];
    Int_std = [Int_std, stdInt];
end

    dlmwrite('raw.txt', raw)
    dlmwrite('Int_avg.txt', Int_avg)
    dlmwrite('Int_std.txt', Int_std)

    % Plot raw integrated intensity
    plot(raw, '-bo');
    title('Intensity profile for each molecule');
    xlabel('Kymograph frame');
    ylabel('Intensity (arbitrary unit)');

    % plot average intensity with standard deviations as errorbars
    %errorbar(Int_avg, Int_std, '-ro');
    %title('Average intensity for each molecule with std error bars');
    %xlabel('Molecule (#)');
    %ylabel('Intensity (arbitrary unit)');

end
```